Modeling sudden cardiac death risks factors in COVID-19 patients -the hydroxychloroquine and azithromycin case

Jérôme Montnach, Isabelle Baró, Flavien Charpentier, Michel de Waard, Gildas Loussouarn

Modeling sudden cardiac death risks factors in COVID-19 patients

– the hydroxychloroquine and azithromycin case

Jérôme Montnach PhD[1], Isabelle Baró PhD[1], Flavien Charpentier PhD[1], Michel De Waard PhD[1,2], Gildas Loussouarn PhD[1*].

1. *Université de Nantes, CNRS, INSERM, l'institut du thorax, F-44000 Nantes, France.*
2. *Laboratory of Excellence « Ion Channels, Science & Therapeutics », F-06560 Valbonne, France.*

*** Address correspondence to:**

Dr. Gildas Loussouarn

L'institut du thorax

INSERM UMR 1087 / CNRS UMR 6291

IRS-UN, 8 Quai Moncousu BP 70721

44007 Nantes cedex 1, France

Tel: +33 (0)2 2808 0150

Fax: +33 (0)2 2808 0130

E-mail: gildas.loussouarn@inserm.fr

Abstract

Aims. Coronavirus disease of 2019 (COVID-19) has rapidly become a worldwide pandemic. Many clinical trials have been initiated to fight the disease. Among those, hydroxychloroquine and azithromycin had initially been suggested to improve clinical outcomes. Despite any demonstrated beneficial effects, they are still in use in some countries but have been reported to prolong the QT interval and induce life-threatening arrhythmia. Since a significant proportion of the world population may be treated with such COVID-19 therapies, evaluation of the arrhythmogenic risk of any candidate drug is needed.

Methods Using the O'Hara-Rudy computer model of human ventricular wedge, we evaluate the arrhythmogenic potential of clinical factors that can further alter repolarization in COVID-19 patients in addition to HCQ and AZM such as tachycardia, hypokalemia, and subclinical to mild long QT syndrome.

Results. HCQ and AZM drugs have little impact on QT duration and do not induce any substrate prone to arrhythmia in COVID-19 patients with normal cardiac repolarization reserve. Nevertheless, in every tested condition in which this reserve is reduced, the model predicts larger ECG impairments, as with dofetilide. In subclinical conditions, the model suggests that mexiletine limits the deleterious effects of AZM and HCQ.

Conclusion. By studying the HCQ and AZM co-administration case, we show that the easy-to-use ORd model can be applied to assess the QT-prolongation potential of off-label drugs, beyond HCQ and AZM, in different conditions representative of COVID-19 patients and to evaluate the potential impact of additional drug used to limit the arrhythmogenic risk.

Keywords: COVID-19; QT duration; arrhythmia; predictive model; asymptomatic**.**

What's new?

- O'Hara-Rudy (ORd) computer model can be used to assess, at the ECG level, COVID-19 off-label drug pro-arrhythmic potential in conditions when the repolarization is impaired.
- Patients with impaired repolarization reserve are at high risk of arrhythmias with such treatments.

- ORd model may help select anti-arrhythmic therapy in addition to COVID-19 treatments.

Introduction

The coronavirus disease of 2019 (COVID-19) caused by the Severe Acute Respiratory Syndrome Coronavirus 2 (SARS-CoV-2), and first identified in Wuhan, China, in December 2019, has rapidly become a global pandemic, with more than 69.5 million confirmed cases and over 1,580,000 deaths on December 12, 2020 (WHO COVID-19 Dashboard). The high transmission rate of the virus and the lack of collective immunization and therapy have made it a threat to public health, despite its low morbidity in a large part of the population (1). Pre-existing cardiovascular disease, including cardiac arrhythmias, is associated with a prognosis worsening (2-5). Arrhythmias were reported in 17% of patients affected by COVID-19 and this percentage reaches 44% for patients in intensive care unit (ICU) (2-4). In absence of approved drugs to prevent or treat COVID-19, many clinical trials have been initiated to test the efficiency of drugs already approved for other diseases on this new pathology. Among those, more than 260 focused on hydroxychloroquine (HCQ) (clinicaltrials.gov), a chloroquine (CQ) derivative historically used to treat malaria and autoimmune diseases (6). HCQ has shown potent *in vitro* activity against both SARS-CoV-1 and SARS-CoV-2 (7-9). Two small, non-randomized, open-label clinical trials in France, suggested that the combination of HCQ and azithromycin (AZM) drugs may reduce the viral load of infected patients and improve clinical outcomes (10, 11). Despite accumulation of studies questioning the clinical efficacy of HCQ, the topic remains highly debated (12-17).

HCQ has been occasionally reported to prolong the QT interval on surface ECG and provoke *torsades de pointes* (TdP), a life-threatening arrhythmia (18-22). AZM has been developed for the treatment of respiratory tract infections (23-25) because the related macrolide, erythromycin, induced prolonged QT intervals and TdP. Nevertheless, AZM has been occasionally reported as a triggering factor of QT prolongation (26, 27), arrhythmias (25, 28, 29) and increased risk for sudden death (25, 30, 31). Both HCQ and AZM are categorized as being at '*torsades de pointes*' risk (crediblemeds.org) and their administration is not recommended to patients presenting with congenital long QT syndrome (LQTS) (32). On the other hand, large population studies indicate that AZM use was not associated with

an increased risk of death from cardiovascular causes in a general population of young and middle-aged adults (33), and 85 out-patients treated with HCQ for connective tissue diseases for a minimum of 1 year did not show QTc interval and heart rate different from those in a population of healthy young adults (34). Last, in two recent studies investigating HCQ and AZM treatment of COVID-19 patients, subsets of 9.2% (11/119 patients) and 16% (40/251) of the treated patients presented severely prolonged QTc to values >500 ms, a known marker of high risk of malignant arrhythmia and sudden cardiac death (35, 36). A more recent meta-analysis reported major QTc prolongation above 60 ms in about 13% of the COVID-19 patients treated with both drugs, with an overall considerable heterogeneity, though (37).

In face of this variability, we exploited a computer model of human ventricular wedge to test the arrhythmogenic potential of a combination of several factors: (i) HCQ and/or AZM treatments, (ii) events occurring in COVID-19 patients that can contribute to alter repolarization: hypokalemia, tachycardia, and (iii) subclinical LQTS phenotypes. We chose the O'Hara and Rudy pseudo-ECG computer model, based on non-diseased human ventricular data (38). This model has been previously used and thoroughly validated by many laboratories, including ours, to study cardiac pathophysiological mechanisms in multiple diseases such as inherited and acquired long QT, short QT and Brugada syndrome (39-46). The model was adapted to incorporate off-target effects of HCQ and AZM on cardiac ion currents (27, 47).

Methods

Transmural wedge simulations

We computed the pseudo-ECG using a 1-dimensional model of a transmural wedge consisting in 165 human ventricular myocytes (ORd model) (38). Cells 1–60 were sub-endocardium type, 61–105 were mid-myocardium type, and 106–165 were sub-epicardium type (Supplemental figure 1). The spatially weighted sum of the voltage gradient was determined at a point 2 cm from the sub-epicardium end of a heterogeneous multicellular

fiber, along the fiber axis. The number of computed beats needed to reach convergence in ECG and action potential (AP) mathematical parameters, was determined by following at each beat, computed single cardiomyocyte AP and Ca^{2+} transient evolution at 1000-ms cycle length, starting from the model initial default conditions. Of note, the number of iterations needed to reach steady-state cannot be used to predict the number of action potentials necessary to reach biological steady-state. At first, AP duration decreased and Ca^{2+} transient amplitude increased to reach a constant value at the 250^{th} beat (Supplemental figure 2; https://models.cellml.org/e/71). A value of 300 beats was chosen for all the tested conditions as it reflected stability of the modelling conditions. The healthy condition was modeled at 1000-ms cycle length, and tachycardia was modeled at 700-ms cycle length, that is commonly observed in COVID-19 patients (3) and at 500-ms cycle length.

To model cardiac response of COVID-19 patients with moderate hypokalemia, external K^+ concentration has been decreased from 5.4 to 3.4 mM.

We reasoned that LQTS patients with major alterations in repolarization would not be prescribed QT lengthening compounds. Thus, we operated moderate modifications of the implicated currents to model long QT syndromes. For type 1 LQTS, we reduced the conductance of the slow component of the delayed rectifier K^+ current (I_{Ks}) to 50% of the wild-type condition to mimic moderate loss-of-function of mutated *KCNQ1*-encoded channels, without any dominant negative effect usually associated with severe LQT (48, 49). Similarly, for type 2 LQTS (LQT2), we reduced the conductance of the rapid component of the delayed rectifier K^+ current (I_{Kr}) to 50% of the wild-type condition to mimic moderate loss-of-function (50). For type 3 LQTS (LQT3), we reproduced the consequences of the ΔQKP1507-1509 mutant on *SCN5A*-encoded channel, $Na_v1.5$, with 4-fold increase in the conductance of the late component of the Na^+ current (51, 52).

Effects of 3 µM HCQ have been chosen based on the serum concentration measured in COVID-19 patients treated with 600 mg/day (10). HCQ effects on ion channels have been modeled as follows: 35% decrease of I_{Kr} conductance and 12% decrease of the

conductance of the L-type Ca^{2+} current, $I_{Ca,L}$ (47). For AZM, data on serum concentrations from SARS-Cov2 patients are not available so far. Peak plasma AZM concentrations during oral dosing range from ≈0.4 to 1.1 µmol/L. However, plasma concentrations are misleading, as the drug accumulates within cells, achieving concentrations approaching 900 µmol/L in leukocytes and pulmonary tissue (27). A previous study by the pharmaceutical sponsor, Pfizer Inc., reported similar accumulation of the drug in cardiac cells for mice receiving oral AZM (200 $mg \cdot kg^{-1} \cdot d^{-1}$ for 10 days), with ≈200-fold increase in concentration compared with plasma at day 10 (53). Based on that, Yang *et al.* used an *in vitro* concentration of 50 µM, which seems reasonable to estimate the effect on cardiac currents (27). Of Note, AZM has different effects with regard to acute (instantaneous) or "chronic" 24-hour exposure, regarding the Na^+ current. Acute exposure to AZM was shown to decrease both the peak sodium current and peak L-type calcium current. It also decreases the inward rectifier potassium current I_{K1}, and the delayed potassium currents I_{Kr} and I_{Ks}. In contrast, 24-hour exposure increases the peak and late sodium currents. Unfortunately, the effects of 24-hour exposure AZM on I_{K1}, I_{Kr}, I_{Ks} and the L-type calcium current were not tested in this earlier report (27). Interestingly, even in the case of acute exposure, Yang *et al.* showed an enlargement of QTc duration in mice (see figure 2 of their publication), suggesting that the decrease in L-type calcium current is counterbalanced or even exceeded by the decrease in I_{K1} (I_{Kr} and I_{Ks} being absent in adult mice). Because AZM is administered for several days in the COVID-19 context, we considered only reported 24-hour effects of this compound on ion channels, as follows: 1.8-fold increase in sodium peak current conductance and 2.5-fold increase in late sodium current conductance. Of note, adding the other current alterations, based on their studied acute effects (65% reduction in L-type calcium current, 30% reduction in I_{Kr} and I_{Ks}, 66% reduction in I_{K1}) further increased QT duration (supplemental figure 3). Since the equivalence between acute and 24-hour effects is hypothetical, we chose to keep the condition with the minimal effect (only clearly established 24-hour effect of AZM on sodium channel). This point stresses out the importance of the characterization of longer application (at least 24-hour) of a given molecule on the currents.

State-dependent effects of mexiletine (MEX) were modeled at therapeutic concentration (0.8-2 µg/mL) (54) by a 40% decrease in only the late sodium current conductance (55).

Two antiarrhythmic drugs, that prolong QT interval and have been reported to induce torsades de pointes, were also tested as positive controls. Dofetilide is mostly active on I_{Kr} and I_{to} at about 2 nM corresponding to the free plasma C_{max} concentration (factors applied: 0.45, 0.98, 0.98, 0.85, 0.98, and 0.95 to I_{Kr}, $I_{Ca,L}$, $I_{Na\ fast}$, I_{to}, I_{Ks} and I_{K1} conductances, respectively) (55). Quinidine has a larger spectrum and was tested at its free plasma C_{max} concentration of about 850 nM (factors applied: 0.3, 0.9, 0.98, 0.85, 0.9, and 0.95 to I_{Kr}, $I_{Ca,L}$, $I_{Na\ fast}$, I_{to}, I_{Ks} and I_{K1} conductances, respectively) (55).

Combined effects (such as LQT mutation+AZM+HCQ+MEX) were obtained by applying each factor respective of each drug or condition to the appropriate conductance(s). Models were processed with C++ code.

Electrophysiological determinations

Pseudo-ECG time parameters were determined as previously described (56). As expected, this model adapts to frequency by decreasing QT duration when frequency increases (38).

As presented above, pseudo-ECG models are obtained from 1-dimensional strand of 165 cells reporting left ventricle transmural activity. For example, apex-to-base and right ventricle-to-left ventricle gradients are absent in this model. Therefore, generated pseudo-ECG time parameters are lower than human ECG values. QRS and QT durations are 46 and 312 ms, respectively, in this model compared to 90-100 and 370-440 ms in patients (*i.e.* -60 ms), suggesting that difference in QT between the model and patients is mainly due to the difference in QRS, not ST duration. For the sake of comparison, we arbitrarily added the empirical value of 60 ms to the model QT duration to obtain 'clinical-like' QT values (in figure 7). QRS widening induced by HCQ may occur in COVID-19 patients. It is a slight median increase of 4 ms of borderline significance (57). However, we kept this 60-ms value constant in every tested condition.

Arrhythmogenic risks were assessed by the repolarization time from APD_{30} to APD_{90} (APD_{90-30}) measured from the beginning of AP upstroke until 30% and 90% of repolarization as

previously described (58) and by QT duration (59). The breaks in the repolarization slope in early phase 3 of the computed APs were considered as early afterdepolarizations (EADs) by analogy with the EAD originally defined as a depolarizing afterpotential that begins prior to the completion of repolarization and causes (or constitutes) an interruption or retardation of normal repolarization, in the *princeps* publication by Cranefield (60). Data were analyzed using R3.6.2 and GraphPad8.

Results

We started with the most general case of COVID-19 patients, presenting no arrhythmia risk factor that reduces the repolarization reserve. Thus, we first investigated the effects of HCQ or AZM alone and their combined effects on the ventricular repolarization on simulated 'normal' ECG. At a cycle length of 1,000 ms, we observed that AZM alone induced a shortening of the QRS complex (-24%) and an increase in QT duration (+7%) due to the increased contribution of the peak and late sodium currents, respectively (Figure 1A-B and Table 1). HCQ alone induced a larger increase in QT duration (+21% *vs*. baseline) without affecting the QRS duration (Figure 1A-B). The combined AZM and HCQ synergistically prolonged the QT interval (30%; figure 1A-B). These drugs target two different types of ion channels. HCQ reduces a repolarizing current (I_{Kr}), while AZM increases a depolarizing current (late I_{Na}). Their effects are thus more than additive on the action potential duration as described by previous studies (61). Looking at specific cell levels, modeled action potentials from sub-endocardium (cell #19), mid-myocardium (cell #84) and sub-epicardium (cell #144) underwent major modifications when the effects of HCQ alone or combined with AZM were simulated (Figure 1C).

Because COVID-19 patients admitted in ICU are frequently tachycardic, we investigated the effects of the treatment at a faster rate (cycle length, CL = 700 ms). The resulting effects of the three treatments on pseudo-ECG and APs parameters were in the same range as at

1,000-ms CL (Figure 2A-B and Table 1). When higher heart rate was tested (CL = 500 ms), similar results were observed (Supplemental figure 4).

Because hypokalemia can precipitate acquired LQTS (62), we investigated AZM and HCQ effects when a moderate hypokalemia (3.4 mM of extracellular K^+) commonly observed in COVID-19 patients (63) was implemented in the model in addition to tachycardia. As shown in Figure 2C, hypokalemia induced a QT prolongation (+5% compared to baseline at 700-ms CL) and exacerbated the effects of the AZM+HCQ combination (+33% of increase in QT compared to +25% of increase in normokalemia at 700-ms CL; figure 2C). Hypokalemia also hyperpolarized the diastolic membrane potential of each cardiomyocyte layer (-99.2 mV in hypokalemia *vs.* -86.9 mV in normokalemia) leading to increased sodium channel availability. This increased availability caused QRS shortening. The combination of both drugs induced a triangulation of the AP shape as assessed by the prolongation of the repolarization time from APD_{30} to APD_{90} (APD_{90-30}; 195 ms *vs.* 110 ms with no treatment, in the sub-endocardium; figure 2D), which is known to favor early afterdepolarizations (64, 65). In summary, the model suggests that COVID-19 patients with tachycardia and hypokalemia, even 'sub-clinical', have to be closely monitored due to the potentiation of HCQ and AZM arrhythmogenic effects.

QT and AP duration lengthening were also observed when the reference drugs dofetilide and quinidine were applied (Supplemental figures 5 and 6). The deleterious effects of well-known arrhythmogenic drugs can be clearly identified. It appears that AZM+HCQ have similar effects as dofetilide, a high risk torsadogenic drug. In summary, our results confirm the AZM+HCQ-induced QT prolongation observed in patients and validate the use of the model to investigate the arrhythmogenic consequences of drugs to treat COVID-19.

In order to validate the use of this model to predict arrhythmogenic susceptibility of patients with moderate long QT syndrome, we first tested AZM and HCQ effects in a LQT2 model

196 replicating hERG haplo-insufficiency in normokalemia. As expected, a 33% prolongation of
197 the QT was obtained. AZM+HCQ combined effects further prolonged it by 21% *vs*.
198 'untreated' LQT2 condition (Figure 3A). In LQT2 conditions, AP repolarization relies mostly
199 on I_{Ks}. As expected, the AZM-HCQ combined effects were major in the mid-myocardium
200 where I_{Ks} is of small amplitude. Mid-myocardium APD_{90-30}, already prolonged by I_{Kr}
201 decrease, was severely prolonged from 145 to 203 ms by AZM+HCQ treatment and
202 associated with the occurrence of a subthreshold early afterdepolarization (Figure 3B).
203 Again, AZM+HCQ treatment had effects in the same range as those observed with dofetilide
204 (Supplemental figures 5 and 6). In the same conditions, quinidine application led to more
205 pronounced QT prolongation and EADs particularly at the mid-myocardium level. These sets
206 of data show that the ORd model replicated the impact of proarrhythmic drugs on LQT2 AP
207 and ECG. These results confirm the absolute proscription of the use of such proarrhythmic
208 drugs in COVID-19 patients with baseline long QT (66-68).

209 Then, we used the model to predict the effects of AZM and HCQ in the context of a sub-
210 clinical QT prolongation as seen in parents of patients with autosomal recessive Jervell and
211 Lange-Nielsen LQTS, for instance (69). Despite a 50% reduction in I_{Ks} amplitude, a minimal
212 3% prolongation of the QT duration was observed (Figure 4A). However, the combination of
213 AZM and HCQ induced a 26% increase in QT duration (vs. 'untreated' LQT1 condition) as
214 well as APD_{90} prolongation (Figure 4). This approach suggests that COVID-19 patients with
215 primary moderate hypokalemia or asymptomatic LQT1 have a slightly higher risk to develop
216 drug-induced arrhythmias when treated with AZM and HCQ than patients without these co-
217 morbidities (+11% and +4% QT prolongation in hypokalemia and LQT1, respectively,
218 compared to QT values of 'treated' 'normal' ECG at the same heart rhythm). These patients
219 have to be followed closely and additional preventive anti-arrhythmic therapy might be
220 proposed in this case.

As AZM increases the late component of the sodium current, we also investigated the effects of the combined therapy in a model in which the late component of the Na^+ current was already increased *i.e*. in the model replicating LQT3. A 13% QT prolongation was obtained, to a lesser extent than in the LQT2 condition, though. However, a dramatic QT prolongation of 44% was induced by AZM+HCQ treatment (Figure 5A). At the 'cellular level', combining both drugs effects favored AP triangulation (APD_{90-30} duration increased from 102 to 195 ms) and occurrence of early afterdepolarizations in mid-myocardium, close to what was obtained with the LQT2 model (Figure 5B).

Since it appears that the ORd model confirmed the observed and expected results regarding HCQ and AZM effects on ECG, we used the model to predict the effect of mexiletine treatment. Mexiletine, a well-known anti-arrhythmic drug used in LQTS patients was proposed to be associated with HCQ and AZM treatment of COVID-19 patients to limit excessive QT prolongation (70, 71). As shown in Figure 6, mexiletine reversed AZM+HCQ-induced QT prolongation in all tested conditions (+19% *vs.* +25% in tachycardia, +22% *vs.*+33% in hypokalemia, +16% *vs.*+21% in LQT2, +20% *vs.*+26% in LQT1, and +28% *vs.*+45% in LQT3 model). In hypokalemia, LQT2 and LQT3 models, mexiletine reduced the AZM+HCQ-induced early afterdepolarization susceptibility in mid-myocardium (APD_{90-30} of 131 ms *vs.*148 ms, 186 ms *vs.* 203 ms and 159 *vs.*195 ms for in hypokalemia, LQT2, and LQT3 models, respectively). Of note, the model predicts that mexiletine supplementation to shorten the prolonged QT has a mild but not negligible effect. Moreover, the model may be robust enough to evaluate the combined effects of new additional drugs (with known effects on ion channels) to limit AZM+HCQ arrhythmogenic consequences.

Figure 7 summarizes the QT duration values obtained at 700-ms cycle length. The ORd transmural wedge model values are arbitrarily transposed to clinical-like values by adding 60 milliseconds (right Y-axis). A QTc cut-off of 500 ms is clinically considered as pathological

(66-68). At 700 ms of cycle length, the corresponding absolute QT duration according to Bazett's formula is 418 ms.

Discussion

Our study confirms that treating COVID-19 patients with HCQ and AZM drugs has, in most patients, little impact on QT duration (72) and does not induce any substrate prone to arrhythmia. However, in clinical conditions in which the repolarization reserve is reduced, the model predicts larger ECG impairments including QT > 418 ms at 700 ms of cycle length, corresponding to QTc > 500 ms (figure 7). Such dramatic QT prolongations are potentially enabling the occurrence of life-threatening events, such as ventricular fibrillation. In addition, the model allows the dissection of the relative contribution of each drug to the establishment of pro-arrhythmic conditions, as well as their synergic effects to the mechanisms involved. We also show that, mexiletine can limit only partly the dramatic increase in QT duration for patients with tachycardia, hypokalemia or reduced conduction reserve, but can bring it back to manageable duration for the mildest phenotypes. These results are in agreement with observations reported by Badri *et al.* after mexiletine treatment on acquired-LQT syndrome patients (73). The use of lidocaine, another class I antiarrhythmic drug has shown some benefits in a COVID-19 patient treated with AZM and HCQ (74). Therefore, the ORd model may be used to evaluate the potential impact of additional drug, with known effects on ion channels, to limit the arrhythmogenic risks.

There is currently an explosion of proposed therapies for treating the virus but none of them have clearly demonstrated their efficacy (75). Among these therapies, hydroxychloroquine combined with azithromycin is still being used based on *in vitro* studies indicating their ability to inhibit virus-cell fusion (7-9) and despite accumulation of studies questioning their clinical efficacy, the topic is still debated (12-16). A major concern of this therapy has been the risk of QT prolongation and TdP. The proarrhythmic mechanism of HCQ is thought to be due to

its ability to inhibit hERG potassium channel and L-type calcium channel, which can result in early afterdepolarization triggered activity (47). Association of well-timed early afterdepolarization and QT prolongation results in TdP. The proarrhythmic mechanism of AZM is thought to be due to its ability to increase cardiac sodium current and promote intracellular sodium loading (27). Obviously, clinical decision cannot rely on the results obtained with this ECG model, but, by comparing the effects obtained with AZM+HCQ, and two proarrhythmic drugs, it can be suspected that the treatment has deleterious effects *in vivo*. Indeed, based on the proposed mechanisms we confirmed, using this *in silico* model, recent reports indicating QT prolongation (72, 76) and high risk of TdP (77) in COVID-19 patients treated with HCQ and/or AZM. The discrepancy between occasional reports of QT prolongation and life-threatening arrhythmias triggered by HCQ and AZM and the absence of QT prolongation effects in large population studies (especially with AZM (33)), is probably due to the necessity, for triggering arrhythmia, of the combination of factors such as tachycardia, hypokalemia, and subclinical LQTS as substrate.

More than 280 drugs have been reported to induce QTc prolongation (78). Among them several are antiarrhythmic drugs, but also non-cardiovascular drugs, that are widely used in ICU (79). Clear recommendations have been established to avoid their administration to patients with symptomatic and well-established congenital long QT syndrome. In addition, I_{Kr}, I_{Ks}, $I_{Ca,L}$, $I_{Na\ late}$ and more generally Ca^{2+} homeostasis, are differentially impaired in various cardiopathies and cardiomyopathies frequently associated with aging, and also in hypoxia, much more frequent conditions in hospitalized COVID-19 patients. This is of concern, especially since $I_{Na\ late}$ increase, most frequently associated with these acquired diseases, appears to lead to severe ECG changes (LQT3).

Regardless of genetic aspects or pre-existing chronic pathologies, clinical case series have also identified risk factors for drug-induced LQTS including hypokalemia as commonly observed in COVID-19 patients (80). Hypokalemia prolongs QT and is a risk factor for drug-

induced LQTS. In addition to direct consequences on I_{Kr} current (81, 82), hypokalemia may activate CaMKII leading to an increase in late sodium current and further prolongation of ventricular repolarization (83). Moderate to severe hypokalemia has been reported in COVID-19 patients (63). SARS-CoV-2 virus invades cells through binding to angiotensin I converting enzyme 2 (ACE2) that enhances ACE2 degradation. The final effect of this degradation is a continuous renal K^+ loss that makes it difficult to correct hypokalemia (63). Noteworthy, low levels of potassium have been correlated with QTc > 500 ms occurrence in COVID-19 patients under HCQ and AZM medication (36). Consistent with these observations, this model emphasizes the fact that kalemia of COVID-19 patients has to be followed very carefully, particularly in case of medication with drugs such as HCQ or AZM. More generally, this model could be used to evaluate in a pre-clinical approach, the risk of drug-induced QT prolongation in this context. In addition to electrolyte imbalance, there is also a greater prevalence of risks factors among COVID-19 patients in ICU, including older age, presence of underlying heart disease, and co-treatment with other QT prolonging medications.

With the possibility that a significant proportion of the world population may receive SARS-CoV-2 drugs with torsadogenic potential, the risk to treat patients with asymptomatic and undiagnosed long QT syndrome is increasing. These patients have a QTc duration in the limit of the general population variability and are not identified as such. Indeed, in a recent study, patients with extreme QTc prolongation when treated with HCQ and AZM, presented a baseline QTc around 431 ms only, within the normal QTc range (36). As modeled in the present study, cardiomyocytes harboring mutations leading to haplo-insufficiency in *KCNQ1* may present very minimal action potential prolongation because of a normal I_{Kr} (84), but I_{Kr} blockers such as HCQ, can lead to marked action potential prolongation in limited repolarization reserve. All guidelines for QT management in COVID-19 context (66-68) recommend to avoid QT prolonging drugs in individuals with a QTc > 500 ms due to a two-fold to three-fold increase in risk for TdP (85). Nevertheless, those asymptomatic patients

might receive these drugs based on this criterion. As modeled in this study, despite the absence of QT prolongation in baseline conditions because of a normal I_{Kr} (84) and regardless of the origin of low repolarization reserve, these patients are at high risk of TdP when I_{Kr} blockers such as HCQ are used. However, the model shows that, in a borderline condition such as moderate LQT1, mexiletine can limit to some extent the deleterious effects of AZM and HCQ. Therefore, we propose that the ORd model can be used to evaluate the potential impact of other additional drugs, with known effects on ion channels, that may be used in the future to limit arrhythmogenic risk of COVID-19 therapies.

In summary, the ORd model appears to be an easy-to-use tool to assess off-label drug arrhythmia potential in different conditions representative of COVID-19 patients at risk for arrhythmia and life-threatening *torsades de pointes*.

Limitations

We used the original ORd model based on its more realistic conductance values compared to others. This model may underestimate I_{Ks} amplitude even if obtained from human cardiomyocytes (86). In some rare cases (heterozygous non-dominant-negative LQT1 mutations) a minimal reduction (less than 50%) of the channel activity leads to severe QTc prolongation (very minor cases, *cf.* for instance (87)). The model we use is simple, robust, and incorporates pseudo ECGs but not inter-individual variability, to remain affordable in time and resources. Since the model does not include the population variability (e.g., due to genetic background), it cannot reproduce the LQTS phenotype heterogeneity. Other studies focusing on single cell AP, adjusted I_{Ks} amplitude to compensate for this insufficiency leading to more severe LQT1 phenotype (88). It would be interesting to try optimizing pseudo-ECG models using the same strategy.

One-dimension strip of 165 cardiomyocytes simulates only the transmural gradient. Apex-to-base and right-to-left gradients are absent in this model. There are 3D models but (i) they

355 are highly computationally demanding thus requiring simpler alternative approaches to
356 model single cell action potential (89) and (ii) they are less realistically adaptive because
357 each current is not individually modelled. Therefore, we preferred to use a 1D-model in
358 which precise biophysical equations representing the biological currents can be finely tuned
359 to model the drug effects at the AP then ECG levels. Thus, the resulting caveat is the lower
360 QT duration values. In order to allow translational approach, we suggest adding an
361 empirically estimated value of 60 ms. The calculated QT values can then be roughly
362 compared to clinical ECG values. In addition, T wave shape results more from regional
363 heterogeneity than from transmural gradients (90). As another limit of the 1D-model, it
364 cannot simulate changes in T wave amplitude.
365 In this study, we investigated potential effects of drugs prescribed to patients with COVID-19
366 on AP with reduced repolarization reserve, in order to detect any arrhythmogenic substrate.
367 To do so, we used well-defined conditions with “pure” repolarization reserve decrease such
368 as LQT syndrome with various genetic origins. Cardiopathies and cardiomyopathies
369 frequently associated with aging, and in hypoxia, are much more frequent conditions in
370 hospitalized COVID-19 patients. However, instead of adding another condition, generic for
371 these pathologies, which is difficult to establish since conductance decreases are not the
372 same for all the pathologies (91), conditions with “pure” repolarization-reserve decrease as
373 LQT syndromes were preferred. Similarly, the complex modifications induced by systemic
374 inflammation and oxidative stress observed in COVID-19 patients have not been introduced
375 at the level of the ion currents in the modeling. Such complex alterations of expression
376 and/or activity of ion channels are hardly quantifiable and cannot be mimicked. In any case,
377 it can be suspected that the addition of pre-existing pathologic conditions and COVID-19-
378 related modifications would exacerbate the arrhythmia susceptibility.
379 The effects of adrenergic stimulation were not evaluated for the following reason. An
380 observational study of 138 patients affected by COVID-19 reported moderate tachycardia
381 with a median heart rate of 88 bpm (3) indicating that the adrenergic tone is not high in those
382 patients. Thus, in this study, we evaluated, during moderate tachycardia, the theoretical

effect of the drugs on AP with reduced repolarization reserve, in order to detect any arrhythmogenic substrate. Interestingly, a very recent work, complementary to ours, used a modified version of the ORd model to study the β-adrenergic receptor stimulation on the cellular proarrhythmic effects of chloroquine and azithromycin, at the single AP level (92). In this paper, Sutanto and Heijman suggest that sympathetic stimulation limits drug-induced APD prolongation. Therefore, at least for CQ and AZM, the unstimulated situation that we studied may represent the most critical situation.

It has to be mentioned that the ECG ORd model is conservative. Arrhythmogenic mechanisms such as triggered activities are hardly induced. Indeed, significant impairment of the Ca^{2+} current window was needed to induce repolarization failure in the recent study of Sutanto and Heijman (92). However, the deleterious effects of arrhythmogenic drugs can be clearly identified with the ECG model, namely EADs and QT lengthening.

Gender differences, resulting from multiple intersecting processes implying complex regulations of ion channels, cannot be easily modeled and was not investigated in this study. This would be indeed another improvement of the model.

Acknowledgments

None

Sources of Funding

M. De Waard and G. Loussouarn thank the Agence Nationale de la Recherche for its financial support to the Région Pays de la Loire (ANR FLASH Covid-19 - CoV2-E-TARGET) and the laboratory of excellence “Ion Channels, Science and Therapeutics” (grant N° ANR-11-LABX-0015). The fellowship of J. Montnach is provided by a National Research Agency Grant to M. De Waard entitled OptChemCom (grant N° ANR-18- CE19-0024-01). Genavie foundation supported J. Montnach and G. Loussouarn.

Disclosures

None

References

1. Chan JF, Yuan S, Kok KH, To KK, Chu H, Yang J, et al. A familial cluster of pneumonia associated with the 2019 novel coronavirus indicating person-to-person transmission: a study of a family cluster. Lancet. 2020;395(10223):514-23.
2. Hulot JS. COVID-19 in patients with cardiovascular diseases. Arch Cardiovasc Dis. 2020;113(4):225-6.
3. Wang D, Hu B, Hu C, Zhu F, Liu X, Zhang J, et al. Clinical Characteristics of 138 Hospitalized Patients With 2019 Novel Coronavirus-Infected Pneumonia in Wuhan, China. JAMA. 2020.
4. Mehra MR, Desai SS, Kuy S, Henry TD, Patel AN. Cardiovascular Disease, Drug Therapy, and Mortality in Covid-19. N Engl J Med. 2020.
5. Izcovich A, Ragusa MA, Tortosa F, Lavena Marzio MA, Agnoletti C, Bengolea A, et al. Prognostic factors for severity and mortality in patients infected with COVID-19: A systematic review. PLoS One. 2020;15(11):e0241955.
6. Ben-Zvi I, Kivity S, Langevitz P, Shoenfeld Y. Hydroxychloroquine: from malaria to autoimmunity. Clin Rev Allergy Immunol. 2012;42(2):145-53.
7. Wang M, Cao R, Zhang L, Yang X, Liu J, Xu M, et al. Remdesivir and chloroquine effectively inhibit the recently emerged novel coronavirus (2019-nCoV) in vitro. Cell Res. 2020;30(3):269-71.
8. Biot C, Daher W, Chavain N, Fandeur T, Khalife J, Dive D, et al. Design and synthesis of hydroxyferroquine derivatives with antimalarial and antiviral activities. J Med Chem. 2006;49(9):2845-9.
9. Yao X, Ye F, Zhang M, Cui C, Huang B, Niu P, et al. In Vitro Antiviral Activity and Projection of Optimized Dosing Design of Hydroxychloroquine for the Treatment of Severe Acute Respiratory Syndrome Coronavirus 2 (SARS-CoV-2). Clin Infect Dis. 2020.
10. Gautret P, Lagier JC, Parola P, Hoang VT, Meddeb L, Mailhe M, et al. Hydroxychloroquine and azithromycin as a treatment of COVID-19: results of an open-label non-randomized clinical trial. Int J Antimicrob Agents. 2020:105949.
11. Gautret P, Lagier JC, Parola P, Hoang VT, Meddeb L, Sevestre J, et al. Clinical and microbiological effect of a combination of hydroxychloroquine and azithromycin in 80 COVID-19 patients with at least a six-day follow up: A pilot observational study. Travel Med Infect Dis. 2020:101663.
12. Uzunova K, Filipova E, Pavlova V, Vekov T. Insights into antiviral mechanisms of remdesivir, lopinavir/ritonavir and chloroquine/hydroxychloroquine affecting the new SARS-CoV-2. Biomedicine & pharmacotherapy = Biomedecine & pharmacotherapie. 2020;131:110668.
13. Prodromos CC. Hydroxychloroquine is protective to the heart, not Harmful: A systematic review. New microbes and new infections. 2020:100747.
14. Ong WY, Go ML, Wang DY, Cheah IK, Halliwell B. Effects of Antimalarial Drugs on Neuroinflammation-Potential Use for Treatment of COVID-19-Related Neurologic Complications. Molecular neurobiology. 2020.
15. Oldenburg CE, Doan T. Azithromycin for severe COVID-19. Lancet. 2020.
16. Albani F, Fusina F, Giovannini A, Ferretti P, Granato A, Prezioso C, et al. Impact of Azithromycin and/or Hydroxychloroquine on Hospital Mortality in COVID-19. Journal of clinical medicine. 2020;9(9).

17. Peng H, Chen Z, Wang Y, Ren S, Xu T, Lai X, et al. Systematic Review and Pharmacological Considerations for Chloroquine and Its Analogs in the Treatment for COVID-19. Front Pharmacol. 2020;11:554172.
18. O'Laughlin JP, Mehta PH, Wong BC. Life Threatening Severe QTc Prolongation in Patient with Systemic Lupus Erythematosus due to Hydroxychloroquine. Case Rep Cardiol. 2016;2016:4626279.
19. Morgan ND, Patel SV, Dvorkina O. Suspected hydroxychloroquine-associated QT-interval prolongation in a patient with systemic lupus erythematosus. J Clin Rheumatol. 2013;19(5):286-8.
20. de Olano J, Howland MA, Su MK, Hoffman RS, Biary R. Toxicokinetics of hydroxychloroquine following a massive overdose. Am J Emerg Med. 2019;37(12):2264 e5-e8.
21. Chen CY, Wang FL, Lin CC. Chronic hydroxychloroquine use associated with QT prolongation and refractory ventricular arrhythmia. Clin Toxicol (Phila). 2006;44(2):173-5.
22. Oscanoa TJ, Vidal X, Kanters JK, Romero-Ortuno R. Frequency of Long QT in Patients with SARS-CoV-2 Infection Treated with Hydroxychloroquine: A Meta-analysis. Int J Antimicrob Agents. 2020;56(6):106212.
23. Owens RC, Jr., Nolin TD. Antimicrobial-associated QT interval prolongation: pointes of interest. Clin Infect Dis. 2006;43(12):1603-11.
24. Kowey PR, Yan GX. Discarding the baby with the bathwater. Pacing and clinical electrophysiology : PACE. 2007;30(12):1429-31.
25. Huang BH, Wu CH, Hsia CP, Yin Chen C. Azithromycin-induced torsade de pointes. Pacing and clinical electrophysiology : PACE. 2007;30(12):1579-82.
26. Sears SP, Getz TW, Austin CO, Palmer WC, Boyd EA, Stancampiano FF. Incidence of Sustained Ventricular Tachycardia in Patients with Prolonged QTc After the Administration of Azithromycin: A Retrospective Study. Drugs Real World Outcomes. 2016;3(1):99-105.
27. Yang Z, Prinsen JK, Bersell KR, Shen W, Yermalitskaya L, Sidorova T, et al. Azithromycin Causes a Novel Proarrhythmic Syndrome. Circ Arrhythm Electrophysiol. 2017;10(4).
28. Tilelli JA, Smith KM, Pettignano R. Life-threatening bradyarrhythmia after massive azithromycin overdose. Pharmacotherapy. 2006;26(1):147-50.
29. Kezerashvili A, Khattak H, Barsky A, Nazari R, Fisher JD. Azithromycin as a cause of QT-interval prolongation and torsade de pointes in the absence of other known precipitating factors. J Interv Card Electrophysiol. 2007;18(3):243-6.
30. Ray WA, Murray KT, Hall K, Arbogast PG, Stein CM. Azithromycin and the risk of cardiovascular death. N Engl J Med. 2012;366(20):1881-90.
31. Mosholder AD, Mathew J, Alexander JJ, Smith H, Nambiar S. Cardiovascular risks with azithromycin and other antibacterial drugs. N Engl J Med. 2013;368(18):1665-8.
32. Naksuk N, Lazar S, Peeraphatdit TB. Cardiac safety of off-label COVID-19 drug therapy: a review and proposed monitoring protocol. Eur Heart J Acute Cardiovasc Care. 2020:2048872620922784.
33. Svanstrom H, Pasternak B, Hviid A. Use of azithromycin and death from cardiovascular causes. N Engl J Med. 2013;368(18):1704-12.
34. Costedoat-Chalumeau N, Hulot JS, Amoura Z, Leroux G, Lechat P, Funck-Brentano C, et al. Heart conduction disorders related to antimalarials toxicity: an analysis of electrocardiograms in 85 patients treated with hydroxychloroquine for connective tissue diseases. Rheumatology (Oxford). 2007;46(5):808-10.

503 35. Saleh M, Gabriels J, Chang D, Kim BS, Mansoor A, Mahmood E, et al. The Effect of
504 Chloroquine, Hydroxychloroquine and Azithromycin on the Corrected QT Interval in Patients
505 with SARS-CoV-2 Infection. Circ Arrhythm Electrophysiol. 2020.
506 36. Chorin E, Wadhwani L, Magnani S, Dai M, Shulman E, Nadeau-Routhier C, et al. QT
507 Interval Prolongation and Torsade De Pointes in Patients with COVID-19 treated with
508 Hydroxychloroquine/Azithromycin. Heart Rhythm. 2020.
509 37. Ayele Mega T, Feyissa TM, Dessalegn Bosho D, Kumela Goro K, Zeleke Negera G. The
510 Outcome of Hydroxychloroquine in Patients Treated for COVID-19: Systematic Review and
511 Meta-Analysis. Can Respir J. 2020;2020:4312519.
512 38. O'Hara T, Virag L, Varro A, Rudy Y. Simulation of the undiseased human cardiac
513 ventricular action potential: model formulation and experimental validation. PLoS Comput
514 Biol. 2011;7(5):e1002061.
515 39. Yang PC, Clancy CE. In silico Prediction of Sex-Based Differences in Human
516 Susceptibility to Cardiac Ventricular Tachyarrhythmias. Front Physiol. 2012;3:360.
517 40. Whittaker DG, Ni H, Benson AP, Hancox JC, Zhang H. Computational Analysis of the
518 Mode of Action of Disopyramide and Quinidine on hERG-Linked Short QT Syndrome in
519 Human Ventricles. Front Physiol. 2017;8:759.
520 41. Tyan L, Foell JD, Vincent KP, Woon MT, Mesquitta WT, Lang D, et al. Long QT
521 syndrome caveolin-3 mutations differentially modulate Kv 4 and Cav 1.2 channels to
522 contribute to action potential prolongation. J Physiol. 2019;597(6):1531-51.
523 42. Tomek J, Tomkova M, Zhou X, Bub G, Rodriguez B. Modulation of Cardiac Alternans
524 by Altered Sarcoplasmic Reticulum Calcium Release: A Simulation Study. Front Physiol.
525 2018;9:1306.
526 43. Portero V, Le Scouarnec S, Es-Salah-Lamoureux Z, Burel S, Gourraud JB, Bonnaud S,
527 et al. Dysfunction of the Voltage-Gated K+ Channel beta2 Subunit in a Familial Case of
528 Brugada Syndrome. J Am Heart Assoc. 2016;5(6).
529 44. Lee HC, Rudy Y, Liang H, Chen CC, Luo CH, Sheu SH, et al. Pro-arrhythmogenic Effects
530 of the V141M KCNQ1 Mutation in Short QT Syndrome and Its Potential Therapeutic Targets:
531 Insights from Modeling. J Med Biol Eng. 2017;37(5):780-9.
532 45. Romero L, Trenor B, Yang PC, Saiz J, Clancy CE. In silico screening of the impact of
533 hERG channel kinetic abnormalities on channel block and susceptibility to acquired long QT
534 syndrome. Journal of molecular and cellular cardiology. 2015;87:271-82.
535 46. Li Z, Dutta S, Sheng J, Tran PN, Wu W, Chang K, et al. Improving the In Silico
536 Assessment of Proarrhythmia Risk by Combining hERG (Human Ether-a-go-go-Related Gene)
537 Channel-Drug Binding Kinetics and Multichannel Pharmacology. Circ Arrhythm
538 Electrophysiol. 2017;10(2):e004628.
539 47. Capel RA, Herring N, Kalla M, Yavari A, Mirams GR, Douglas G, et al.
540 Hydroxychloroquine reduces heart rate by modulating the hyperpolarization-activated
541 current If: Novel electrophysiological insights and therapeutic potential. Heart Rhythm.
542 2015;12(10):2186-94.
543 48. Vanoye CG, Desai RR, Fabre KL, Gallagher SL, Potet F, DeKeyser JM, et al. High-
544 Throughput Functional Evaluation of KCNQ1 Decrypts Variants of Unknown Significance.
545 Circulation Genomic and precision medicine. 2018;11(11):e002345.
546 49. Chouabe C, Neyroud N, Guicheney P, Lazdunski M, Romey G, Barhanin J. Properties
547 of KvLQT1 K+ channel mutations in Romano-Ward and Jervell and Lange-Nielsen inherited
548 cardiac arrhythmias. The EMBO journal. 1997;16(17):5472-9.

549 50. Ng CA, Perry MD, Liang W, Smith NJ, Foo B, Shrier A, et al. High-throughput
550 phenotyping of heteromeric human ether-a-go-go-related gene potassium channel variants
551 can discriminate pathogenic from rare benign variants. Heart Rhythm. 2020;17(3):492-500.
552 51. Shi R, Zhang Y, Yang C, Huang C, Zhou X, Qiang H, et al. The cardiac sodium channel
553 mutation delQKP 1507-1509 is associated with the expanding phenotypic spectrum of LQT3,
554 conduction disorder, dilated cardiomyopathy, and high incidence of youth sudden death.
555 Europace : European pacing, arrhythmias, and cardiac electrophysiology : journal of the
556 working groups on cardiac pacing, arrhythmias, and cardiac cellular electrophysiology of the
557 European Society of Cardiology. 2008;10(11):1329-35.
558 52. Montnach J, Chizelle FF, Belbachir N, Castro C, Li L, Loussouarn G, et al. Arrhythmias
559 precede cardiomyopathy and remodeling of Ca(2+) handling proteins in a novel model of
560 long QT syndrome. Journal of molecular and cellular cardiology. 2018;123:13-25.
561 53. Araujo FG, Shepard RM, Remington JS. In vivo activity of the macrolide antibiotics
562 azithromycin, roxithromycin and spiramycin against Toxoplasma gondii. Eur J Clin Microbiol
563 Infect Dis. 1991;10(6):519-24.
564 54. Mazzanti A, Maragna R, Faragli A, Monteforte N, Bloise R, Memmi M, et al. Gene-
565 Specific Therapy With Mexiletine Reduces Arrhythmic Events in Patients With Long QT
566 Syndrome Type 3. J Am Coll Cardiol. 2016;67(9):1053-8.
567 55. Crumb WJ, Jr., Vicente J, Johannesen L, Strauss DG. An evaluation of 30 clinical drugs
568 against the comprehensive in vitro proarrhythmia assay (CiPA) proposed ion channel panel.
569 J Pharmacol Toxicol Methods. 2016;81:251-62.
570 56. Ledezma CA, Zhou X, Rodriguez B, Tan PJ, Diaz-Zuccarini V. A modeling and machine
571 learning approach to ECG feature engineering for the detection of ischemia using pseudo-
572 ECG. PLoS One. 2019;14(8):e0220294.
573 57. Mazzanti A, Briani M, Kukavica D, Bulian F, Marelli S, Trancuccio A, et al. Association
574 of Hydroxychloroquine With QTc Interval in Patients With COVID-19. Circulation.
575 2020;142(5):513-5.
576 58. Hondeghem LM, Carlsson L, Duker G. Instability and triangulation of the action
577 potential predict serious proarrhythmia, but action potential duration prolongation is
578 antiarrhythmic. Circulation. 2001;103(15):2004-13.
579 59. Elming H, Holm E, Jun L, Torp-Pedersen C, Kober L, Kircshoff M, et al. The prognostic
580 value of the QT interval and QT interval dispersion in all-cause and cardiac mortality and
581 morbidity in a population of Danish citizens. European heart journal. 1998;19(9):1391-400.
582 60. Cranefield PF. Action potentials, afterpotentials, and arrhythmias. Circulation
583 research. 1977;41(4):415-23.
584 61. Virag L, Acsai K, Hala O, Zaza A, Bitay M, Bogats G, et al. Self-augmentation of the
585 lengthening of repolarization is related to the shape of the cardiac action potential:
586 implications for reverse rate dependency. British journal of pharmacology.
587 2009;156(7):1076-84.
588 62. El-Sherif N, Turitto G, Boutjdir M. Acquired Long QT Syndrome and Electrophysiology
589 of Torsade de Pointes. Arrhythm Electrophysiol Rev. 2019;8(2):122-30.
590 63. chen d, Li X, song q, Hu C, Su F, Dai J. Hypokalemia and Clinical Implications in
591 Patients with Coronavirus Disease 2019 (COVID-19). 2020.
592 64. Guo D, Zhao X, Wu Y, Liu T, Kowey PR, Yan GX. L-type calcium current reactivation
593 contributes to arrhythmogenesis associated with action potential triangulation. Journal of
594 cardiovascular electrophysiology. 2007;18(2):196-203.

595 65. Grant AO, Tranquillo J. Action potential and QT prolongation not sufficient to cause
596 Torsade de Pointes: role of action potential triangulation. Journal of cardiovascular
597 electrophysiology. 2007;18(2):204-5.
598 66. Giudicessi JR, Noseworthy PA, Friedman PA, Ackerman MJ. Urgent Guidance for
599 Navigating and Circumventing the QTc-Prolonging and Torsadogenic Potential of Possible
600 Pharmacotherapies for Coronavirus Disease 19 (COVID-19). Mayo Clin Proc. 2020.
601 67. Roden DM, Harrington RA, Poppas A, Russo AM. Considerations for Drug Interactions
602 on QTc in Exploratory COVID-19 (Coronavirus Disease 2019) Treatment. Circulation. 2020.
603 68. Wu CI, Postema PG, Arbelo E, Behr ER, Bezzina CR, Napolitano C, et al. SARS-CoV-2,
604 COVID-19 and inherited arrhythmia syndromes. Heart Rhythm. 2020.
605 69. Schulze-Bahr E, Haverkamp W, Wedekind H, Rubie C, Hordt M, Borggrefe M, et al.
606 Autosomal recessive long-QT syndrome (Jervell Lange-Nielsen syndrome) is genetically
607 heterogeneous. Hum Genet. 1997;100(5-6):573-6.
608 70. Giudicessi JR, Roden DM, Wilde AAM, Ackerman MJ. Genetic susceptibility for
609 COVID-19-associated sudden cardiac death in African Americans. Heart Rhythm.
610 2020;17(9):1487-92.
611 71. Carpenter A, Chambers OJ, El Harchi A, Bond R, Hanington O, Harmer SC, et al.
612 COVID-19 Management and Arrhythmia: Risks and Challenges for Clinicians Treating
613 Patients Affected by SARS-CoV-2. Front Cardiovasc Med. 2020;7:85.
614 72. Mercuro NJ, Yen CF, Shim DJ, Maher TR, McCoy CM, Zimetbaum PJ, et al. Risk of QT
615 Interval Prolongation Associated With Use of Hydroxychloroquine With or Without
616 Concomitant Azithromycin Among Hospitalized Patients Testing Positive for Coronavirus
617 Disease 2019 (COVID-19). JAMA Cardiol. 2020.
618 73. Badri M, Patel A, Patel C, Liu G, Goldstein M, Robinson VM, et al. Mexiletine Prevents
619 Recurrent Torsades de Pointes in Acquired Long QT Syndrome Refractory to Conventional
620 Measures. JACC Clin Electrophysiol. 2015;1(4):315-22.
621 74. Mitra RL, Greenstein SA, Epstein LM. An algorithm for managing QT prolongation in
622 coronavirus disease 2019 (COVID-19) patients treated with either chloroquine or
623 hydroxychloroquine in conjunction with azithromycin: Possible benefits of intravenous
624 lidocaine. HeartRhythm case reports. 2020;6(5):244-8.
625 75. Kupferschmidt K, Cohen J. Race to find COVID-19 treatments accelerates. Science.
626 2020;367(6485):1412-3.
627 76. Chorin E, Dai M, Shulman E, Wadhwani L, Bar-Cohen R, Barbhaiya C, et al. The QT
628 interval in patients with COVID-19 treated with hydroxychloroquine and azithromycin.
629 Nature Medicine. 2020.
630 77. Szekely Y, Lichter Y, Shrkihe BA, Bruck H, Oster HS, Viskin S. Chloroquine-induced
631 torsade de pointes in a COVID-19 patient. Heart Rhythm. 2020.
632 78. Woosley RL, Black K, Heise CW, Romero K. CredibleMeds.org: What does it offer?
633 Trends Cardiovasc Med. 2018;28(2):94-9.
634 79. Etchegoyen CV, Keller GA, Mrad S, Cheng S, Di Girolamo G. Drug-induced QT Interval
635 Prolongation in the Intensive Care Unit. Curr Clin Pharmacol. 2017;12(4):210-22.
636 80. Roden DM. Predicting drug-induced QT prolongation and torsades de pointes. J
637 Physiol. 2016;594(9):2459-68.
638 81. Yang T, Roden DM. Extracellular potassium modulation of drug block of IKr.
639 Implications for torsade de pointes and reverse use-dependence. Circulation.
640 1996;93(3):407-11.

641 82. Yang T, Snyders DJ, Roden DM. Rapid inactivation determines the rectification and
642 [K+]o dependence of the rapid component of the delayed rectifier K+ current in cardiac
643 cells. Circulation research. 1997;80(6):782-9.
644 83. Pezhouman A, Singh N, Song Z, Nivala M, Eskandari A, Cao H, et al. Molecular Basis of
645 Hypokalemia-Induced Ventricular Fibrillation. Circulation. 2015;132(16):1528-37.
646 84. Roden DM, Viswanathan PC. Genetics of acquired long QT syndrome. J Clin Invest.
647 2005;115(8):2025-32.
648 85. Schwartz PJ, Woosley RL. Predicting the Unpredictable: Drug-Induced QT
649 Prolongation and Torsades de Pointes. J Am Coll Cardiol. 2016;67(13):1639-50.
650 86. Virag L, Iost N, Opincariu M, Szolnoky J, Szecsi J, Bogats G, et al. The slow component
651 of the delayed rectifier potassium current in undiseased human ventricular myocytes.
652 Cardiovasc Res. 2001;49(4):790-7.
653 87. Biliczki P, Girmatsion Z, Brandes RP, Harenkamp S, Pitard B, Charpentier F, et al.
654 Trafficking-deficient long QT syndrome mutation KCNQ1-T587M confers severe clinical
655 phenotype by impairment of KCNH2 membrane localization: evidence for clinically
656 significant IKr-IKs alpha-subunit interaction. Heart Rhythm. 2009;6(12):1792-801.
657 88. Mann SA, Imtiaz M, Winbo A, Rydberg A, Perry MD, Couderc JP, et al. Convergence
658 of models of human ventricular myocyte electrophysiology after global optimization to
659 recapitulate clinical long QT phenotypes. Journal of molecular and cellular cardiology.
660 2016;100:25-34.
661 89. Lopez-Perez A, Sebastian R, Ferrero JM. Three-dimensional cardiac computational
662 modelling: methods, features and applications. Biomed Eng Online. 2015;14:35.
663 90. Janse MJ, Coronel R, Opthof T. Counterpoint: M cells do not have a functional role in
664 the ventricular myocardium of the intact heart. Heart Rhythm. 2011;8(6):934-7.
665 91. Aiba T, Tomaselli GF. Electrical remodeling in the failing heart. Curr Opin Cardiol.
666 2010;25(1):29-36.
667 92. Sutanto H, Heijman J. Beta-Adrenergic Receptor Stimulation Modulates the Cellular
668 Proarrhythmic Effects of Chloroquine and Azithromycin. Front Physiol. 2020;11:587709.

669

670

671 **Figure 1: Hydroxychloroquine/azithromycin-induced prolongation of ventricular**
672 **repolarization in a healthy heart (wedge *in silico* model). A.** Computed pseudo-ECG in
673 control (black), azithromycin (AZM, blue), hydroxychloroquine (HCQ, orange) and
674 AZM+HCQ (red) condition at 1000-ms of cycle length (CL). **B.** QT interval measured in each
675 condition. **C.** Left: Simulation of ventricular action potential from sub-endocardium (top), mid-
676 myocardium (middle) and sub-epicardium (bottom) in control, AZM, HCQ and AZM+HCQ
677 condition. Right: Quantification of action potential duration at 30% (APD_{30}), 50% (APD_{50}),
678 70% (APD_{70}) and 90% (APD_{90}) of repolarization in each condition.

Figure 2: Hydroxychloroquine/azithromycin combination effects in COVID-19 patient model with tachycardia and hypokalemia. A. Tachycardia, (a) computed pseudo-ECG in control (black), azithromycin (AZM, blue), hydroxychloroquine (HCQ, orange) and AZM+HCQ (red) condition at 700-ms of cycle length. (b) QT interval measured in each condition. **B.** (a) Simulation of ventricular action potential from sub-endocardium (left), mid-myocardium (middle) and sub-epicardium (right) in control, AZM, HCQ and AZM+HCQ condition. (b) Quantification of action potential duration at 30% (APD_{30}), 50% (APD_{50}), 70% (APD_{70}) and 90% (APD_{90}) of repolarization in each condition. **C.** Hypokalemia, (a) computed pseudo-ECG in control (dashed black line), hypokalemia (3.4 mM extracellular K^+, solid black line) and hypokalemia with AZM+HCQ (red) condition at 700 ms of cycle length. (b) QT interval measured in each condition. **D.** (a) Simulation of ventricular action potential from sub-endocardium (left), mid-myocardium (middle) and sub-epicardium (right) in control, hypokalemia and hypokalemia with AZM+HCQ condition. (b) Quantification of action potential duration as in B(b), in each condition.

Figure 3: Arrhythmogenic effects of AZM+HCQ combination in long QT type 2 model. A. (a) Computed pseudo-ECG in control (dashed black line), long QT type 2 (LQT2) modeled as a *KCNH2* haploinsufficiency (solid black line) and LQT2 with AZM+HCQ (red) condition at 700-ms of cycle length. (b) QT interval measured in each condition. **B.** (a) Simulation of ventricular action potential from sub-endocardium (left), mid-myocardium (middle) and sub-epicardium (right) in control, LQT2, and LQT2 with AZM+HCQ condition. *: subthreshold early afterdepolarization. (b) Quantification of action potential duration at 30% (APD_{30}), 50% (APD_{50}), 70% (APD_{70}) and 90% (APD_{90}) of repolarization in each condition.

Figure 4: Hydroxychloroquine/azithromycin combination reveals arrhythmia susceptibility in asymptomatic long QT type 1 model. A. (a) Computed pseudo-ECG in control (dashed black line), long QT type 1 (LQT1) modeled as a *KCNQ1* haploinsufficiency (solid black line) and LQT1 with AZM+HCQ (red) condition at 700-ms of cycle length. (b) QT

interval measured in each condition. **B.** (a) Simulation of ventricular action potential from sub-endocardium (left), mid-myocardium (middle) and sub-epicardium (right) in control, LQT1 and LQT1 with AZM+HCQ condition. (b) Quantification of action potential duration at 30% (APD_{30}), 50% (APD_{50}), 70% (APD_{70}) and 90% (APD_{90}) of repolarization in each condition.

Figure 5: Arrhythmogenic effects of AZM+HCQ combination in long QT type 3 model. **A.** (a) Computed pseudo-ECG in control (dashed black line), long QT type 3 (LQT3) modeled as a 4-fold increase in persistent sodium current (solid black line) and LQT3 with AZM+HCQ (red) condition at 700-ms of cycle length. (b) QT interval measured in each condition. **B.** (a) Simulation of ventricular action potential from sub-endocardium (left), mid-myocardium (middle) and sub-epicardium (right) in control, LQT3 and LQT3 with AZM+HCQ condition. *: subthreshold early-afterdepolarization. (b) Quantification of action potential duration at 30% (APD_{30}), 50% (APD_{50}), 70% (APD_{70}) and 90% (APD_{90}) of repolarization in each condition.

Figure 6: Mexiletine partially limits AZM+HCQ-induced QT prolongation. Combination of mexiletine with AZM+HCQ (purple) limits increase in QT interval in pseudo ECG (a) and simulated ventricular action potential (b) prolongation in tachycardia (**A**), hypokalemia (**B**), LQT1 (**C**), LQT2 (**D**) and LQT3 (**E**) conditions compared to the same condition without mexiletine (red).

Figure 7: ORd model QT transposed to clinical human QT. In all conditions, converted AZM+HCQ QT values exceed (right Y-axis) the 418 ms cut-off (dashed line) and the use of mexiletine allows a partial reversion close to the cut-off value in tachycardia alone or combined with hypokalemia or LQT1 condition.

Table 1. Drugs effects on pseudo-ECG parameters

	QRS (ms)							QT (ms)						
	Basal	+AZM	+HCQ	+AZM + HCQ	+AZM + HCQ + MEX	+Dof.	+Quinidine	Basal	+AZM	+HCQ	+AZM + HCQ	+AZM + HCQ + MEX	+Dof.	+Quinidine
Control	46	35	46	35	35	*n.d.*	*n.d.*	312	333	378	407	382	*n.d.*	*n.d.*
Tachycardia	47	35	47	35	35	50	48	297	310	352	372	353	410	470
HypoK	40	*n.d.*	*n.d.*	32	32	40	40	311	*n.d.*	*n.d.*	414	378	395	461
LQT1	46	*n.d.*	*n.d.*	35	35	50	48	307	*n.d.*	*n.d.*	388	368	433	506
LQT2	46	*n.d.*	*n.d.*	35	35	50	48	394	*n.d.*	*n.d.*	478	457	512	587
LQT3	46	*n.d.*	*n.d.*	35	35	50	48	337	*n.d.*	*n.d.*	487	433	466	538

AZM: azithromycin ; HCQ: hydroxychloroquine ; MEX: mexiletine ; HypoK: hypokalemia; Dof. : dofetilide ; Control at 1000 ms cycle length and other conditions at 700 ms cycle length.

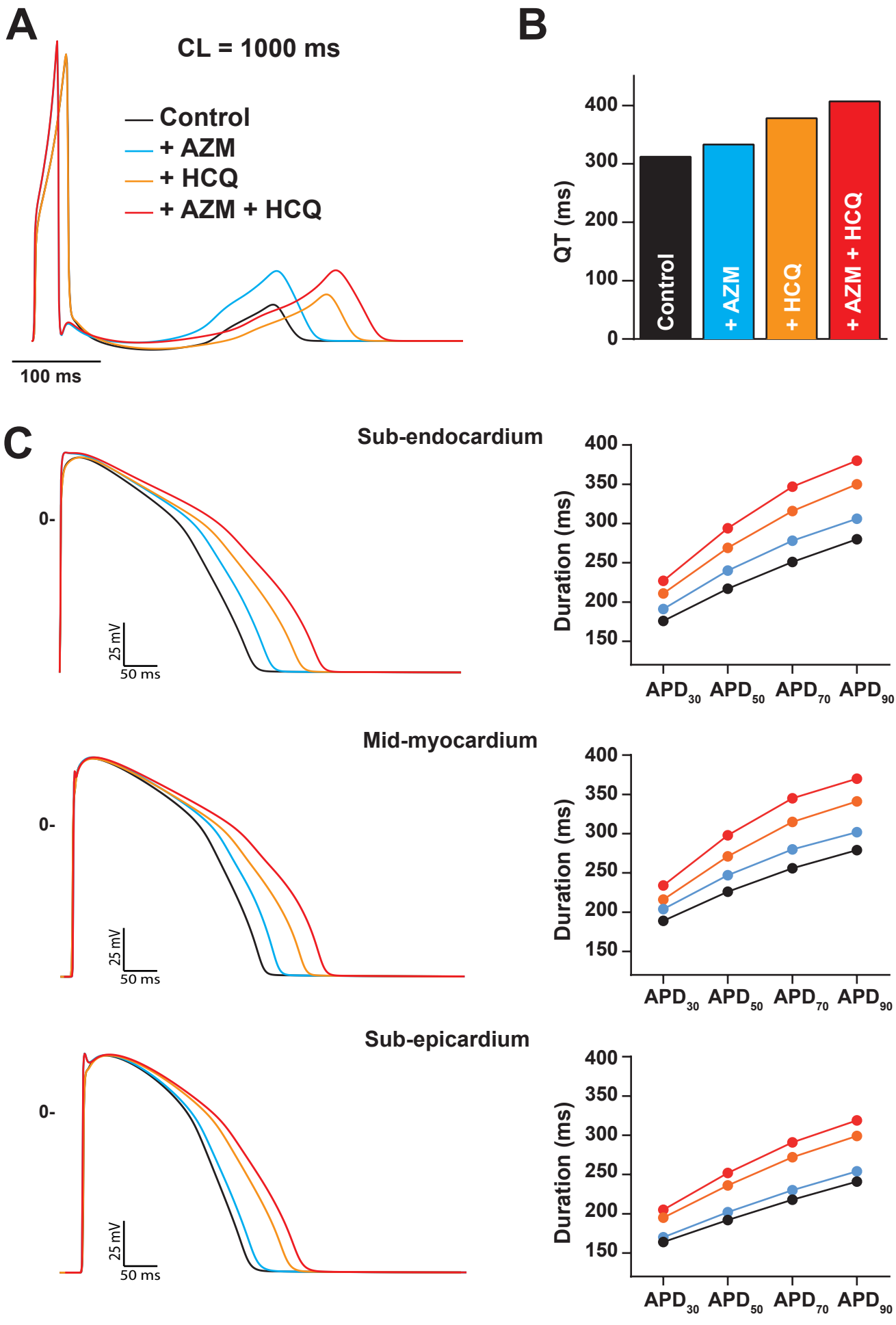
A
CL = 1000 ms
Control
+ AZM
+ HCQ
+ AZM + HCQ
100 ms
B
QT (ms)
400
300
200
100
0
Control
+ AZM
+ HCQ
+ AZM + HCQ
C
Sub-endocardium
0-
25 mV
50 ms
Duration (ms)
400
350
300
250
200
150
APD30 APD50 APD70 APD90
Mid-myocardium
0-
25 mV
50 ms
Duration (ms)
400
350
300
250
200
150
APD30 APD50 APD70 APD90
Sub-epicardium
0-
25 mV
50 ms
Duration (ms)
400
350
300
250
200
150
APD30 APD50 APD70 APD90

Figure 1

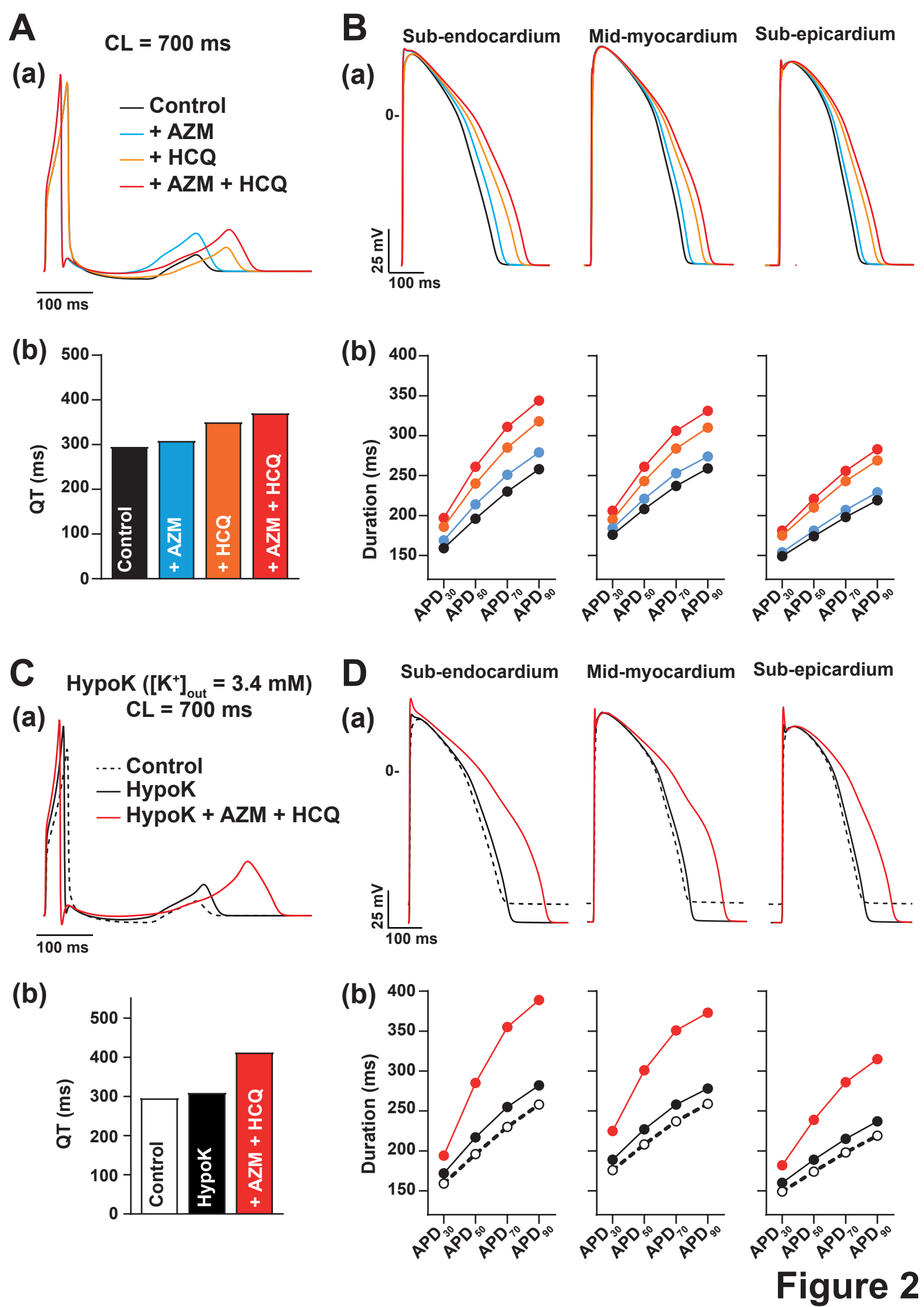
A
CL = 700 ms
(a)
Control
+ AZM
+ HCQ
+ AZM + HCQ
100 ms
B
Sub-endocardium
Mid-myocardium
Sub-epicardium
(a)
0
25 mV
100 ms
(b)
QT (ms)
500
400
300
200
100
0
Control
+ AZM
+ HCQ
+ AZM + HCQ
(b)
Duration (ms)
400
350
300
250
200
150
APD30
APD50
APD70
APD90
C
HypoK ([K+]out = 3.4 mM)
CL = 700 ms
(a)
Control
HypoK
HypoK + AZM + HCQ
100 ms
D
Sub-endocardium
Mid-myocardium
Sub-epicardium
(a)
0
25 mV
100 ms
(b)
QT (ms)
500
400
300
200
100
0
Control
HypoK
+ AZM + HCQ
(b)
Duration (ms)
400
350
300
250
200
150
APD30
APD50
APD70
APD90

Figure 2

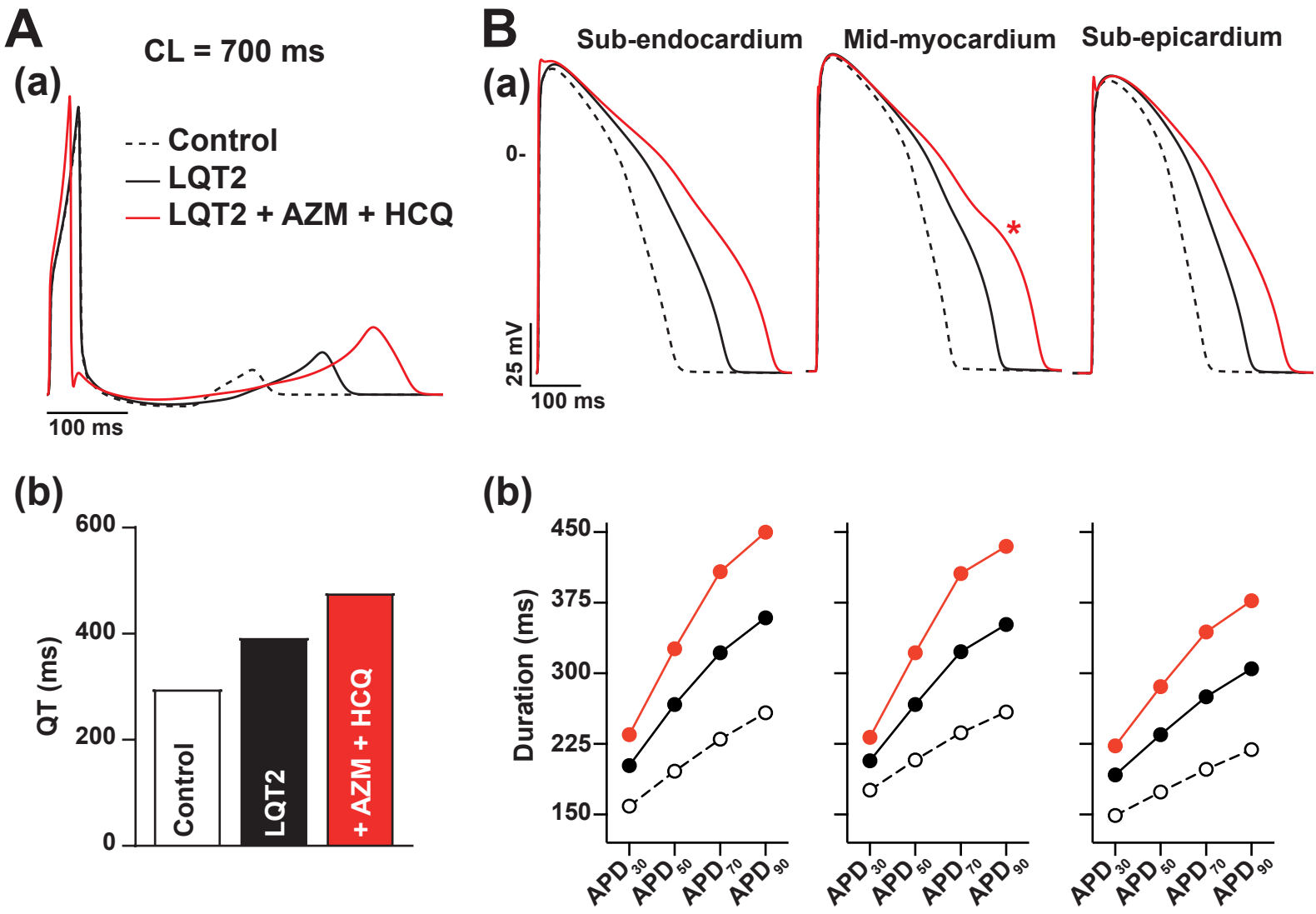
A
(a)
CL = 700 ms
Control
LQT2
LQT2 + AZM + HCQ
100 ms
B
(a)
Sub-endocardium
Mid-myocardium
Sub-epicardium
0-
25 mV
100 ms
*
(b)
QT (ms)
600
400
200
0
Control
LQT2
+ AZM + HCQ
(b)
Duration (ms)
450
375
300
225
150
APD30
APD50
APD70
APD90

Figure 3

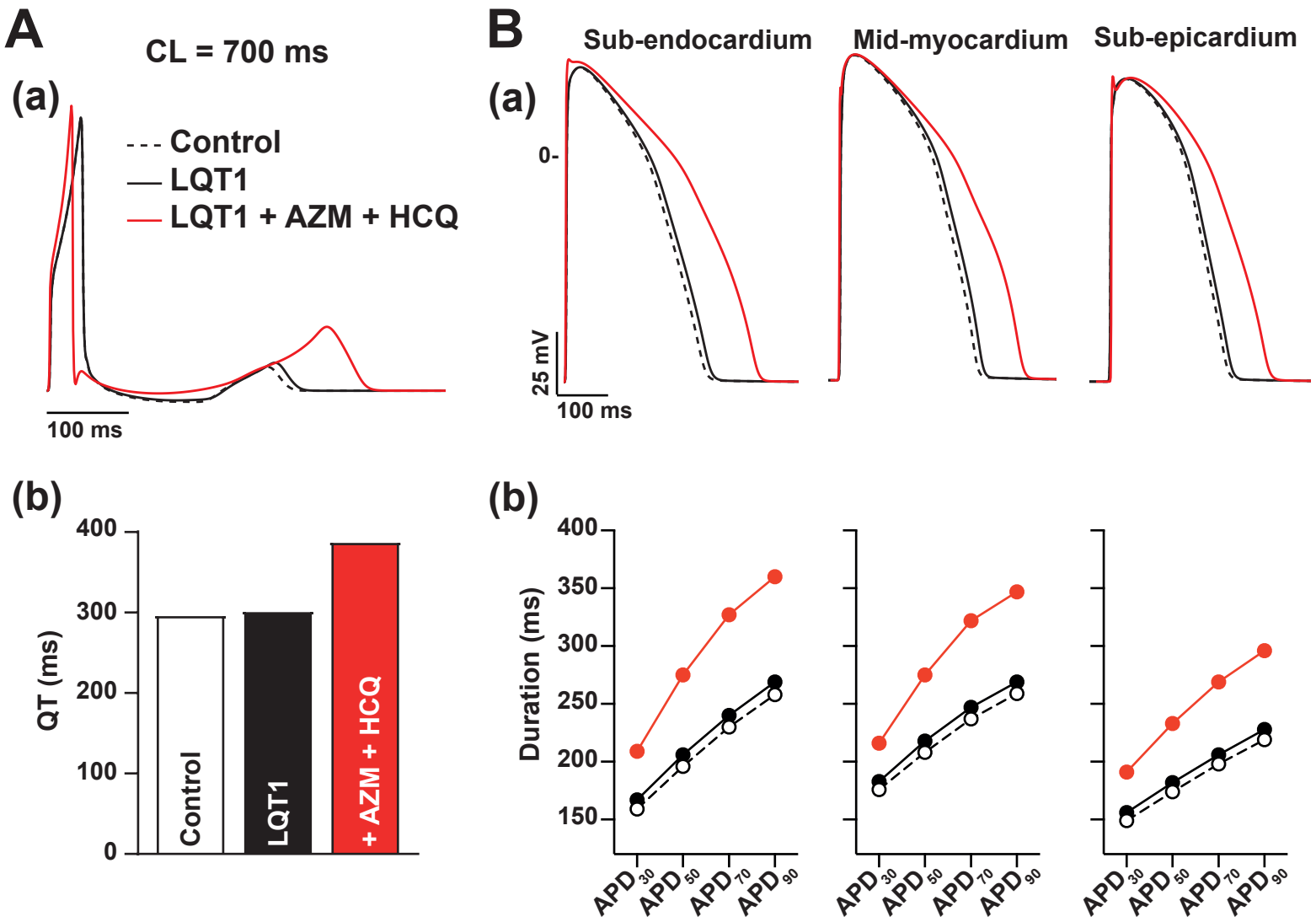
A
CL = 700 ms
(a)
Control
LQT1
LQT1 + AZM + HCQ
100 ms
B
Sub-endocardium
Mid-myocardium
Sub-epicardium
(a)
0-
25 mV
100 ms
(b)
QT (ms)
400
300
200
100
0
Control
LQT1
+ AZM + HCQ
(b)
Duration (ms)
400
350
300
250
200
150
APD30
APD50
APD70
APD90

Figure 4

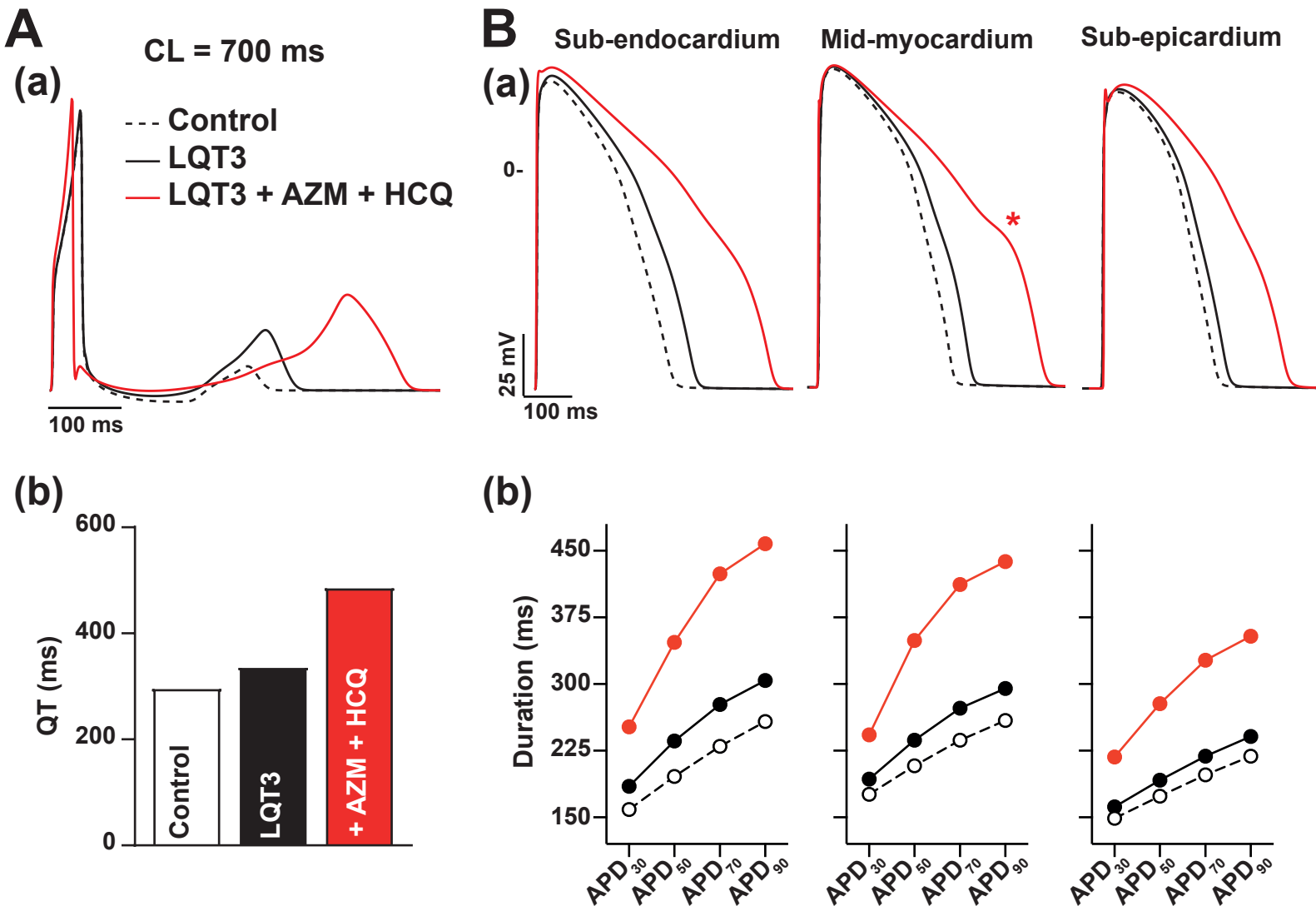
A
(a)
CL = 700 ms
Control
LQT3
LQT3 + AZM + HCQ
100 ms
B
(a)
Sub-endocardium
Mid-myocardium
Sub-epicardium
0-
25 mV
100 ms
*
(b)
QT (ms)
600
400
200
0
Control
LQT3
+ AZM + HCQ
(b)
Duration (ms)
450
375
300
225
150
APD30
APD50
APD70
APD90

Figure 5

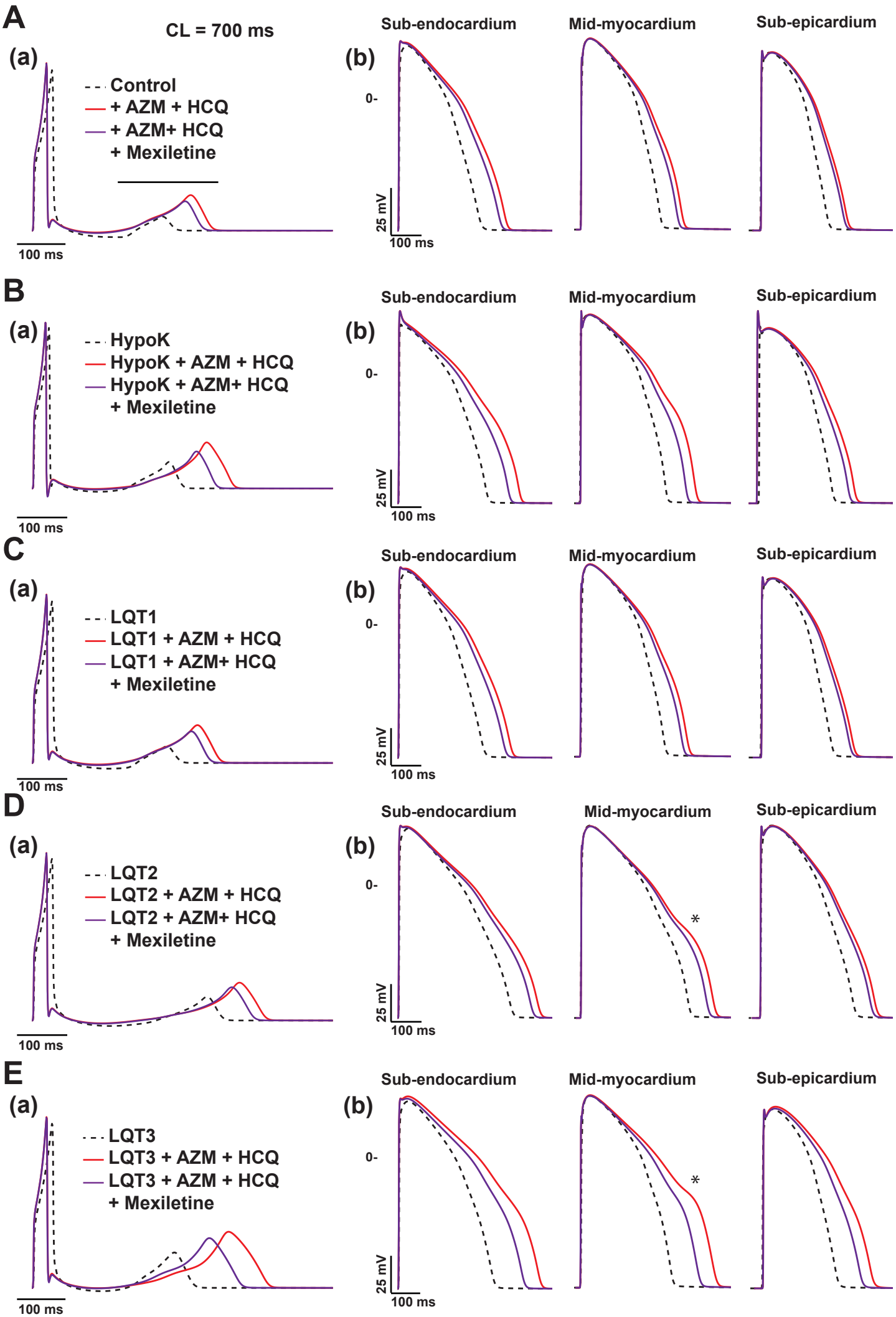
A
CL = 700 ms
(a)
Control
+ AZM + HCQ
+ AZM+ HCQ
+ Mexiletine
100 ms
(b)
Sub-endocardium
Mid-myocardium
Sub-epicardium
0-
25 mV
100 ms
B
(a)
HypoK
HypoK + AZM + HCQ
HypoK + AZM+ HCQ
+ Mexiletine
100 ms
(b)
Sub-endocardium
Mid-myocardium
Sub-epicardium
0-
25 mV
100 ms
C
(a)
LQT1
LQT1 + AZM + HCQ
LQT1 + AZM+ HCQ
+ Mexiletine
100 ms
(b)
Sub-endocardium
Mid-myocardium
Sub-epicardium
0-
25 mV
100 ms
D
(a)
LQT2
LQT2 + AZM + HCQ
LQT2 + AZM+ HCQ
+ Mexiletine
100 ms
(b)
Sub-endocardium
Mid-myocardium
Sub-epicardium
0-
*
25 mV
100 ms
E
(a)
LQT3
LQT3 + AZM + HCQ
LQT3 + AZM + HCQ
+ Mexiletine
100 ms
(b)
Sub-endocardium
Mid-myocardium
Sub-epicardium
0-
*
25 mV
100 ms

Figure 6

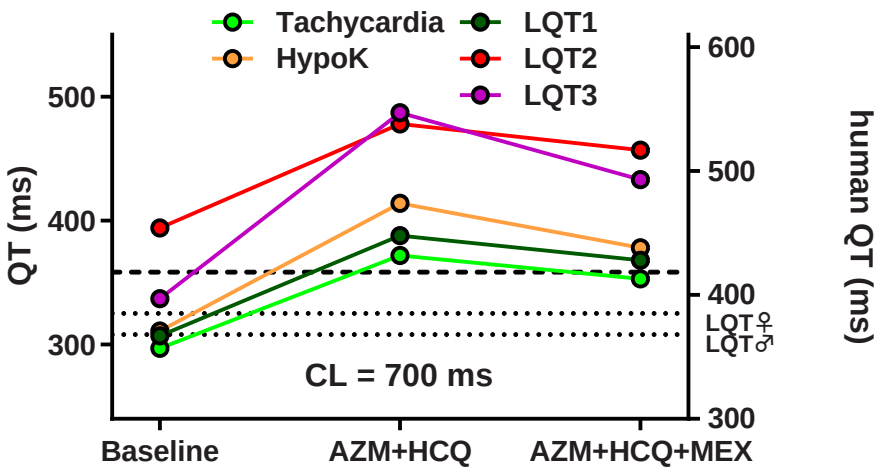
Tachycardia
HypoK
LQT1
LQT2
LQT3
QT (ms)
500
400
300
600
500
400
300
LQT♀
LQT♂
CL = 700 ms
Baseline
AZM+HCQ
AZM+HCQ+MEX
human QT (ms)

Figure 7